Published in final edited form as:
Clin Cancer Res. 2012 January 1; 18(1): 290–300. doi:10.1158/1078-0432.CCR-11-2260.

TP53 disruptive mutations lead to head and neck cancer treatment failure through inhibition of radiation-induced senescence

Heath D. Skinner[1], **Vlad C. Sandulache**[2,3], **Thomas J. Ow**[2], **Raymond E. Meyn**[1], **John S. Yordy**[4], **Beth M. Beadle**[1], **Alison L. Fitzgerald**[2], **Uma Giri**[1], **K. Kian Ang**[1], and **Jeffrey N. Myers**[2]

[1]Department of Radiation Oncology, The University of Texas MD Anderson Cancer Center, Houston, TX

[2]Department of Head and Neck Surgery, The University of Texas MD Anderson Cancer Center, Houston, TX

[3]Bobby R. Alford Department of Otolaryngology - Head and Neck Surgery, Baylor College of Medicine, Houston, TX

[4]The Department of Radiation Oncology, The University of Texas Southwestern Medical Center

Abstract

Purpose—Mortality of patients with head and neck squamous cell carcinoma (HNSCC) is primarily driven by tumor cell radioresistance leading to locoregional recurrence (LRR). In this study, we use a classification of *TP53* mutation (disruptive vs. nondisruptive) and examine impact on clinical outcomes and radiation sensitivity.

Experimental Design—Seventy-four patients with HNSCC treated with surgery and postoperative radiation and 38 HNSCC cell lines were assembled; for each, *TP53* was sequenced and *in vitro* radioresistance measured using clonogenic assays. p53 protein expression was inhibited using shRNA and over-expressed using a retrovirus. Radiation-induced apoptosis, mitotic cell death, senescence, and ROS assays were performed. The effect of the drug metformin on overcoming mutant p53-associated radiation resistance was examined *in vitro* as well as *in vivo*, using an orthotopic xenograft model.

Results—Mutant *TP53* alone was not predictive of LRR; however, disruptive *TP53* mutation strongly predicted LRR (p=0.03). Cell lines with disruptive mutations were significantly more radioresistant (p<0.05). Expression of disruptive *TP53* mutations significantly decreased radiation-induced senescence, as measured by SA-beta-gal staining, p21 expression, and release of reactive oxygen species (ROS). The mitochondrial agent metformin potentiated the effects of radiation in the presence of a disruptive *TP53* mutation partially via senescence. Examination of our patient cohort showed that LRR was decreased in patients taking metformin.

Conclusions—Disruptive *TP53* mutations in HNSCC tumors predicts for LRR, due to increased radioresistance via the inhibition of senescence. Metformin can serve as a radiosensitizer for HNSCC with disruptive *TP53*, presaging the possibility of personalizing HNSCC treatment.

Address for correspondence and reprints: Jeffrey N. Myers, MD, Ph.D., Professor, Head & Neck Surgery, University of Texas MD Anderson Cancer Center, 1515 Holcombe Blvd., Unit 1445, Houston, TX 77030, Phone: (713) 745-2667, Fax: (713) 794-4662, jmyers@mdanderson.org.

Keywords

p53; radiation; senescence; mitotic catastrophe; metformin

Introduction

Head and neck squamous cell carcinoma (HNSCC) is the 6th leading cause of cancer worldwide, with an estimated 49,260 diagnoses each year in the United States alone (1). Although multimodality therapy is important in the management of HNSCC, the eradication of locoregional disease in the primary or postoperative setting is primarily achieved by external beam radiation. As the vast majority of patient deaths from HNSCC are due to locoregional recurrence (LRR), the survival of the patient largely depends upon the radiosensitivity the tumor. Unfortunately, there are few biomarkers to determine radioresistance in HNSCC.

One candidate biomarker is *TP53*, which encodes the p53 protein and is the most commonly altered gene in HNSCC, as demonstrated most recently by our group and others through whole exomic sequencing of a large panel of HNSCC tumors (2). *TP53* has been previously investigated as a biomarker for LRR following radiotherapy in HNSCC with mixed results (3–6). A possible explanation for this finding is mutation-specific functionality of the p53 protein. One large study classifying *TP53* mutations in HNSCC described *TP53* mutation as “disruptive” or “nondisruptive” based upon alteration of DNA binding (7). Any mutation in either the L2 or L3 loop of the DNA binding domain, resulting in a polarity change within the protein, or any stop codon was classified as disruptive. In that study, the presence of a disruptive mutation was associated with poor survival in a heterogeneously treated patient population. Other studies have examined alternative classifications of *TP53*, which were also prognostic of survival in HNSCC (8; 9). Despite these results, there has been little study of the relationship between *TP53* classification and LRR following radiotherapy.

The role of *TP53* in *in vitro* radiosensitivity is also an area of active investigation much of the prior studies producing contradictory results (10–16). Radiation is known to result in p53 activation and apoptosis; however, the contribution of radiation-induced apoptosis to tumor response is not clear, and there are strong arguments that, for most tumor cells, apoptosis plays a minimal role in radiation response (17; 18). In contrast, it has been suggested that mitotic death is the primary mechanism of radiation-induced cell death (19). In this process, abnormal cell division due to DNA damage leads to the formation of large cells with multiple micronuclei (20). It is unclear whether this form of cell death is associated with *TP53* (21–24). Furthermore, emerging data suggest that senescence may play a role in the radiation response, which in some models is dependent upon wild type *TP53* (25). Regardless, the role of *TP53* in radiosensitivity is far from clear.

To investigate the role of *TP53* in radiosensitivity, the current study was performed to determine if a classification of *TP53* (wild type, nondisruptive, or disruptive mutation) predicts for radiosensitivity *in vitro* as well as in the clinical setting. Furthermore, we wished to determine the mechanisms involved in the observed radiation response *in vitro* and use this knowledge to preferentially radiosensitize HNSCC cells.

Methods

Clinical samples

All clinical studies reported in this study have been approved by the University of Texas MD Anderson Cancer Center Institutional Review Board. Seventy-four snap-frozen, pre-

treatment tumor samples were collected from patients with HNSCC at high risk for LRR treated with surgical resection and postoperative radiotherapy from 1992–2003. DNA was extracted from tumor samples, and *TP53* was sequenced (exon 2–12) using Sanger sequencing as described previously (Ow et al, submitted). Mutations were then classified as according to the method of Poeta and colleagues (7). Patients were evaluated every 2–3 months for 1 year following treatment, every 3–4 months the following year, and every 6 months thereafter.

Cell culture and constructs

HNSCC cells were cultured in a 37° C incubator at 5% CO2 for this study as described previously (26). Cells stably expressing short hairpin RNA specific for p53 (shp53) were generated as described previously (27). Briefly, after infection with GFP tagged empty lentiviral vector (LVTHM) or encoding a short-hairpin RNA against p53 (LVUH-shp53) (Addgene, Cambridge, MA), cells were cultured for several passages, and then sorted using flow cytometry. GFP-positive cells were cultured normally. *TP53* constructs (C176F, R282W, R175H and E336X) were generated by extracting RNA from cell lines known to express these mutants. RT-PCR was then performed using *TP53* specific primers. The resulting product was purified and inserted into a pBabe retroviral vector containing a puromycin resistance insert (pBabe-puro) (Addgene, Cambridge, MA) using standard cloning techniques. The resulting vectors were verified by Sanger sequencing at the MD Anderson Cancer Center DNA core facility. After transfection and packaging in 293T cells, viral supernatant was centrifuged at 1,000 rpm to remove cellular debris and added to UMSCC1 cells in combination with polybrene. After one passage, the cells underwent selection with puromycin. All cell lines used in this study have been authenticated against the parental recipient cell line via STR analysis.

Clonogenic assay

HNSCC cells were seeded in 12 well plates at predetermined densities for different radiation doses to allow for an approximately equal number of resultant colonies. The next day, cells were irradiated using a high dose rate ^{137}Cs irradiator (4.5 Gy/min) and cultured for 10–14 days to allow for colony formation. Cells were then fixed in a 3% crystal violet/10% formalin solution. Colonies of >50 cells were then counted and survival fraction was determined. All treatments were in triplicate or greater. For metformin (Sigma-Aldrich, St. Louis, MO) or z-Vad-fmk (BD Pharmingen, San Diego, CA) treatment, cells were pre-treated for 2h prior to radiation with either drug or vehicle (PBS and DMSO respectively) and drug treatment continued overnight. For N-acetyl cysteine (NAC) treatment, the cells were treated starting 2 hours following radiation and drug treatment continued overnight. The cells were then washed and cultured in fresh media for the remainder of the experiment.

Immunofluorescence

HNSCC cells were plated on coverslips and treated as indicated. Cells were washed twice with PBS and fixed using a 1:1 mixture of methanol and acetone for 10 minutes. Cells were then washed in TBS-Tween (TBST) and permeabilized using 0.1% Triton-X for 5 minutes. Cells were again washed with TBST and incubated with FITC-Phalloidin for 1 hour at room temperature. Cells were washed with TBST and mounted on standard glass slides using DAPI-Vectashield (Vector Labortories, Burlingame, CA). For assessment of mitotic death, the number of cells with one or more micronucleus per high power field (hpf) were counted and reported as a percentage of total cells per field. Images were taken from five quadrants, in duplicate, and pooled.

SA-beta-gal staining

Senesence Associated (SA)-beta-gal staining was performed per the manufacturer's instructions (Cell signaling, Danvers, MA). Briefly, HNSCC cells were plated in 6 well plates were irradiated with 4–6 Gy on the next day. Cells were cultured normally until the indicated times post treatment. Cells were then fixed for 10 minutes and stained overnight for SA-beta-gal activity at 37° C. Blue staining cells were scored as senescent and reported as a percentage of all the cells observed per high power field.

Annexin V staining

Annexin V stain was performed per the manufacturer's instructions (BD Pharmingen, San Diego, CA). Briefly, HNSCC cells were cultured normally and treated as indicated. Media was collected, and adherent cells were briefly trypsinized and added to the previously collected media. The cells were then centrifuged, supernatant was removed, and the cells were washed in PBS. The cells were then re-suspended in Annexin V binding buffer, and Annexin V and 7-AAD was added. Samples were mixed gently and incubated at RT. Samples were then analyzed for Annexin V and 7-AAD staining using a Beckman Coulter XL 4 color cytometer (Beckman Coulter, Brea, CA), and the data were analyzed using Flo-Jo software (FloJo, Ashland, OR). Early apoptosis was determined by the proportion of cells that were Annexin V positive and 7-AAD negative.

Cell cycle analysis

HNSCC cells were seeded in a 6 well plate and incubated for the indicated time. Media was collected; cells were washed twice in PBS and trypsinized. The resulting cell suspension was washed in PBS and fixed with 70% ethanol at room temperature for 30 minutes. Cells were then washed in PBS and stained with propidium iodide. Cell cycle detection was then performed using a Beckman Coulter XL 4 color cytometer, (Beckman Coulter, Brea, CA) and the data were analyzed using Flo-Jo software (FloJo, Ashland, OR).

Reactive oxygen species (ROS) measurement

Intra-cellular ROS levels were measured according to previously published protocols using 5-(and-6)-carboxy-2′,7′-dichlorofluorescein (CM-H2DCFDA) dye(28). Briefly, cells were loaded with CM-H2DCFDA for 60 minutes in culture media. Media was changed prior to irradiation to remove excess dye. Fluorescence was measured at various times following irradiation using a standard spectrophotometer, normalized to the control condition and total amount of DNA (29). For flow cytometric experiments, cells were incubated with CM-H2DCFDA dye as described and trypsinized, and fluorescence was analyzed using flow cytometry as described above.

Immunoblotting

Cells were treated as indicated and washed three times with cold PBS. Standard lysis buffer was then added to each plate and incubated on ice for 15 minutes. Cells were then collected using a plastic scraper and centrifuged at 14,000 rpm at 4° C for 10 minutes. The supernatant was removed, and total protein concentration was then calculated using Bio-Rad protein assay (Bio-Rad, Hercules, CA). Immunoblot analysis was performed as described previously (26). Membranes were blocked for 1 hour at RT using 1% powdered milk in 0.1% Tween 20 in Tris-buffered saline, then incubated overnight with either anti-p53 DO-1 (Santa Cruz Biotechnology, CA), anti-β actin (Cell signalling, Danvers, MA), or anti-p21 (BD Pharmingen, San Diego, CA) at 4° C. The following day, membranes were washed with 0.1% Tween 20 in Tris-buffered saline and incubated for 1 hour at RT with species-specific secondary antibody. For p53 and actin, fluorescently conjugated secondary antibodies (Invitrogen, Carlsbad, CA) were used and signal was analyzed using an odyssey

infrared imaging system (LI-COR Biosciences, Lincoln, NE) and associated software (v3.0). For p21, horseradish peroxidase conjugated anti-rabbit immunoglobulin G (Santa Cruz Biotechnology, Santa Cruz, CA) was used and signal was generated using the SuperSignal West chemiluminescent system (Pierce Biotechnology, Rockford, IL).

p21 transcription

Induction of p21 transcription was measured via luciferase reporter activity using a vector containing the 2.4 kb p21 promoter and firefly luciferase (pWWP-Luc)(30) (Addgene, Cambridge, MA). UMSCC1 (p53 null) cells expressing various *TP53* constructs were co-transfected with pWWp-Luc and a constitutively active Renilla luciferase construct using Liopfectamine 2000 (Introgen, Carlsbad, CA). Cells were irradiated the following day at the indicated doses and incubated for 24 hours prior to collection. Luciferase activity was measured using the Promega Dual-Luciferase assay system (Madison, WI).

Orthotopic mouse model

All animal experimentation was approved by the University of Texas MD Anderson Cancer Center Animal Care and Use Committee (ACUC). The orthotopic mouse model has been previously described (31). Briefly, mice were injected with 100,000 HN 31 cells in the anterior half of the oral tongue on Day 0. Once tumor growth was noted, tumors were treated with radiation using a Co^{60} irradiator and custom lead blocks (5 Gy) on Day 8 post-injection and/or metformin (250mg/kg daily, intra-peritoneal). Each treatment group consisted of a total of 10 mice. Mice received a total of 8 daily metformin treatments over the experimental period. Tumor measurements were obtained on Days 6, 13, 16, and 20 post-injection. Tumor volume was calculated as previously described (31).

Statistics

LRR and overall survival (OS) for the patient population was calculated using the Kaplan-Meier method, and comparisons between groups were determined using log rank statistics. Multivariate analysis for LRR was performed using forward step-wise Cox regression analysis. Variables included: tumor and nodal stage, surgical margin status or extracapsular extension, site, gender, smoking history, and *TP53* status. ANOVA with post-hoc analysis or student's t-tests were performed to analyze *in vitro* data and tumor volume. All p values are 2-sided. P values less than 0.05 were considered significant.

Results

Disruptive TP53 mutations are associated with increased LRR following PORT

Disruptive *TP53* is associated with decreased survival in HNSCC, which we hypothesized was due to higher rates of LRR following PORT. To explore this hypothesis, we sequenced *TP53* in HNSCC tumors from 74 patients treated with PORT. Patient characteristics were similar between different *TP53* classification groups (Supplemental Table 1). Median follow-up of surviving patients was 154 months (range 82–185). No significant difference in LRR was found between patients with wild type *TP53* and any mutant *TP53* (Figure 1A). However, classification of *TP53* as disruptive, nondisruptive, or wild type, demonstrated that disruptive *TP53* is an independent predictor of LRR on multivariate analysis (p=0.022). Patients with disruptive *TP53* had a 5 year freedom from LRR of 41% compared to 64% and 76% in patients with wild type and nondisruptive *TP53*, respectively (p=0.03, Figure 1B). No significant difference in LRR was seen between patients with wild type and nondisruptive *TP53* (p=0.48, Figure 1B). Similarly, the OS rates for patients in this study were predicted by *TP53* classification. Specifically, 5 year OS for patients with disruptive

TP53 mutations was 19% compared to 52% in patients with wild type *TP53* and 41% in patients with nondisruptive *TP53* (p=0.031).

Disruptive TP53 mutations are associated with p53-mediated radioresistance

The finding that disruptive *TP53* mutations are associated with a high rate of LRR led to the hypothesis that HNSCC tumor cells with disruptive *TP53* are intrinsically more radioresistant. To test this hypothesis, we evaluated the radiosensitivity of a panel of 38 HNSCC cell lines of known *TP53* status (Supplemental Table 3) and found that cell lines harboring disruptive *TP53* mutations were significantly more radioresistant than those with either nondisruptive or wild type *TP53* (Figure 2A).

To determine if this observed correlation was due to p53 expression, p53 was silenced using stably expressed short hairpin RNA (shp53) in the following HNSCC cell lines: i) UMSCC1 17A and HN 30 (wild type *TP53*), ii) Detroit (R175H, nondisruptive *TP53*), and iii) HN 31 (C176F) and FADU (R248L) (disruptive *TP53*). Inhibition of p53 expression in cell lines expressing wild type or nondisruptive *TP53* rendered cells more radioresistant (Figure 2B & Supplemental Table 2). However, inhibition of p53 expression in cell lines expressing disruptive *TP53* rendered these cells more radiosensitive (Figure 2D & Supplemental Table 2). Conversely, UMSCC1 cells, which have no endogenous p53, were engineered to express either: i) wild type *TP53*, ii) nondisruptive *TP53* (R175H, R282W), or iii) disruptive *TP53* (C176F, E336X). Disruptive *TP53* expressing UMSCC1 cells were found to be radioresistant relative to wild type *TP53* and nondisruptive *TP53* expressing cells (Figure 2C & Supplemental Table 2).

Alteration of p53 expression does not affect radiation-induced mitotic death or apoptosis

To explore the means by which disruptive *TP53* mutation confers radioresistance in HNSCC cells, we evaluated several modes of cellular response to radiation. Initially we examined mitotic death, thought to be one of the primary modes of cell death following radiation(19). Mitotic death, as measured by the presence of micronuclei, was significant following radiation, with all HNSCC cell lines tested exhibiting mitotic death in 20–30% of irradiated cells. However there was no correlation between micronuclei formation, *TP53* expression, and relative radiosensitivity (Supplemental Figure 2).

Furthermore, when either annexin V or sub-G1 staining were analyzed, neither of these measures of apoptosis were related to *TP53* status (Supplemental Figure 3). In fact, only a very small proportion of apoptotic cells were observed (~1–5%), even in those cells shown to be radiosensitive in the clonogenic survival assay. As radiation-induced apoptosis is thought to be caspase-dependent(32), we also treated cells with a pan-caspase inhibitor (Z-vad-fmk) to determine the role of apoptosis in this model. Inhibition of caspase activity had almost no effect on clonogenic survival following radiation (Supplemental Figure 3), supporting to the hypothesis that apoptosis does not play a major role in the radiation response.

Radiation robustly induces SA-beta-gal activity in HNSCC cells which is strongly associated with TP53 status and correlates with clonogenic survival

In cells with wild type or nondisruptive *TP53*, treatment with radiation resulted in a decrease in the proportion of cells in S phase and a less prominent G1 arrest (Supplemental Figure 4). Furthermore, inhibition of p53 expression in HN 30 (wild type *TP53*) cells partially abrogated the observed inability to progress through S phase. Because this phenomenon has been previously linked to cellular senescence, we hypothesized a role for altered senescence in the observed differences in radiosensitivity. To evaluate for cellular senescence, cells were treated with radiation and stained for the SA-beta-gal. As shown in Figure 3, radiation

treatment led to significant levels of SA-beta-gal activity in cell lines expressing either wild type (HN 30) or nondisruptive mutant *TP53* (Detroit, R175H). Furthermore, in these cells with SA-beta-gal staining, the morphologic characteristics of cellular senescence were observed, specifically a large, flattened cell with the classic “fried egg” appearance on microscopy. Inhibition of p53 expression in both of these cell lines significantly reduced levels of radiation-induced SA-beta-gal activity. However, in HN 31 (C176F, disruptive *TP53*) cells, which have disruptive *TP53* and are otherwise isogenic with the HN 30 (wild type *TP53*) cell line, inhibition of p53 expression was associated with elevated levels of radiation-induced SA-beta-gal activity. Forced expression of wild type, as well as two nondisruptive *TP53* mutations (R175H and R282W) in p53 null cells, increased radiation-induced SA-beta-gal activity; conversely, expression of disruptive *TP53* mutations (C176F and E336X) led to decreased SA-beta-gal activity compared to empty vector control (Figure 3B). Furthermore, in experiments comparing micronuclei formation and SA-beta-gal staining in the same cell, the main differences between cells of different *TP53* statuses appear to be within the cells staining positive for SA-beta-gal alone (Figure 3D).

The effects of TP53 status on radiation-induced SA-beta-gal activity are correlated with p21 expression and mediated by ROS production

In addition to SA-beta-gal activity, senescence has been previously linked to induction of p21 expression and ROS production, both of which are believed to be necessary for maintenance of the senescent phenotype (33–36). To determine if radiation-induced p21 expression correlates with *TP53* classification, we assayed p21 protein levels following radiation in cell lines expressing representative *TP53* mutations. In cells expressing wild type *TP53* or a nondisruptive *TP53* mutation, p21 protein and reporter activity were induced by radiation treatment (Figure 4A). In contrast, cells expressing disruptive *TP53* (C176F) had no induction of p21.

ROS also play a key role in senescence and radiation effect. In the current study, radiation-induced ROS levels correlated with p21 expression, SA-beta-gal activity, and relative radiosensitivity. Specifically, ROS were most highly induced in cells which had greater levels of radiation induced SA-beta-gal activity (wild type and R175H), with little or no ROS induction was seen in cells with disruptive *TP53* (C176F) (Figure 4B). Inhibition of ROS using N-acetyl cysteine (NAC) 2 hours following radiation treatment, designed to inhibit secondary ROS production following the initial radiation insult, dramatically decreased senescence in cell lines with normally high levels of radiation-induced SA-beta-gal, but had no effect on cells with disruptive *TP53* (Figure 4C). These results closely correlated with the observed effects of NAC on clonogenic survival following radiation (Figure 4D).

Metformin preferentially potentiates the effects of radiation in HNSCC cells partially via increased senescence

Based on the combined morphologic appearance of irradiated cells, the presence of SA-beta-gal staining, the characteristic induction of p21 and ROS, and the lack of apoptosis, cells with either wild type or non-disruptive *TP53* mutation appear to be undergoing radiation-induced senescence, while cells with a disruptive *TP53* mutation are not. Because the induction of senescence may be clinically beneficial, we wished to investigate drug based therapies designed to this end. As there are no specific senescence inducing agents currently available, we examined metformin, an anti-diabetic agent with minimal clinical toxicity, that has been shown to both induce ROS in some cellular contexts (37) as well preferentially target cell lines with mutant *TP53* (38). In the current study, concurrent radiation and metformin treatment was active against HNSCC cell lines that harbored disruptive *TP53* (Supplemental Figure 5). Conversely, no effect of metformin was seen in cells expressing

wild type *TP53* (HN 30 and MCF-7). Also, the addition of metformin dramatically increased ROS in HN 31 cells, which have a disruptive (C176F) *TP53* mutation, but had much less effect in HN 30 cells, their wild type *TP53* isogenic counterpart (Supplemental Figure 5). Similarly, metformin decreased clonogenic survival following radiation and increased radiation-induced SA-beta-gal activity in HN 31 cells (C176F, disruptive *TP53*), but had little effect in HN 30 cells (wild type *TP53*) (Figure 5A & B). Furthermore, after inhibition of wild type p53 expression, metformin was found to potentiate SA-beta-gal activity and decrease clonogenic survival (Figure 5A & B).

Given the above findings, we examined the effect of metformin treatment on tumor response to radiation in an orthotopic model of HNSCC described previously (26; 31). As seen in Figure 5C, the addition of metformin to radiation dramatically decreased tumor growth compared to either radiation alone (p=0.015) or metformin alone (p=0.008).

To further investigate the clinical utility of metformin, a cohort of patients treated with PORT for HNSCC was identified and the impact of concurrent metformin use was investigated. In addition to the patients in the current study, an additional 30 patients with similar disease characteristics and treatment as well as known *TP53* status were evaluated. Although only 10 patients were taking metformin at the time of radiation, these patients had a dramatically lower LRR rate compared to controls matched for tumor and nodal stage, surgical margin status, and *TP53* status (p=0.04, Figure 5D). On multivariate analysis controlling for *TP53* classification, tumor stage, and surgical margin positivity, metformin use was significantly associated with decreased LRR (p=0.04) as well as improved OS (p=0.01). Specifically, 5 year OS was 87% in the patients taking metformin compared to 41% in the remaining patients (p=0.04).

Discussion

In HNSCC, the majority of patient deaths result from LRR, with up to 60–75% dying of their disease (39). The primary method of treating advanced HNSCC involves radiation, either in the definitive or postoperative setting. To date, there are few clinically useful predictive indicators of LRR following radiotherapy. In the current study, we examined LRR in HNSCC and, for the first time, demonstrated that the disruptive classification of *TP53* is predictive of poor response to a specific therapy, namely PORT. Interestingly, mutant *TP53* alone was not predictive for LRR, arguing for the use of a TP53 mutation classification scheme that can demonstrate differential function between *TP53* mutants in regards to radioresistance.

Because the goal of PORT is to eradicate microscopic residual disease, we hypothesized that LRR would primarily result from intrinsically radioresistant cells. To investigate this, we utilized an *in vitro* approach, combining silencing of endogenous p53 expression with genetically engineered expression of different *TP53* mutations; this approach demonstrated that HNSCC cells with disruptive *TP53* exhibited a radioprotective effect of p53 expression, arguing for a “gain of function” (GOF) in regards to radiosensitivity. These GOF mutations in *TP53* have been shown previously for other cellular processes; however, this report is one of the first to do so for *in vitro* radiosensitivity. Furthermore, we found that two types of cell death most commonly associated with radiation, namely apoptosis and mitotic death, were either not present and/or unaffected by *TP53* status. In fact, the main response to radiation affected by *TP53* status in this model was cellular senescence.

Senescence is a form of cell arrest in which cells remain metabolically active, but lack replicative potential. Several recent studies have linked response to chemotherapy and radiation to this process; however, the exact role of senescence in the response to radiation is

far from clear (17; 40; 41). In the current study, we found radiation-induced senescence correlated strongly with *in vitro* radiosensitivity and was inhibited in the presence of a disruptive *TP53* mutant, again arguing for a GOF by at least a subset of *TP53* mutations within the disruptive category, driving resistance to radiotherapy.

Induction of both p21 and ROS appear to be critical mediators of cellular senescence. Induction of p21 alone can lead to increased ROS production (34), and ROS inhibition can reverse senescence in this context. Conversely, ROS have been linked to induction of p21, and a feedback loop between ROS and p21 is proposed to be required for DNA damage-induced senescence (35; 42; 43).

In the current model, we found radiation-induced ROS and p21 only in HNSCC cells with wild type and nondisruptive *TP53*. Specifically, p21 expression was increased in response to radiation in the context of the nondisruptive *TP53* mutation R175H. Previously, R175H has been shown to have little remnant p53 driven transcription (44; 45). Furthermore, in one report, the disruptive mutation, C176F, has been shown to have some p53 dependent transcriptional activity in a yeast based assay (45); however, this has not been observed in other studies (46; 47). Nevertheless, in the current model, both protein expression and transcription of p21 is induced by radiation in cells expressing either wild type or R175H *TP53*. This could be due to p53 transcription *independent* induction of p21 similar to that seen in other models (48; 49) or it could result from residual p53 transcriptional activity. It has been shown recently that only a small subset of p53 transcriptional targets are necessary for induction of senescence; thus, even a small remnant of transcriptional function may be sufficient (50). Further studies are in progress to discern the mechanism behind this phenomenon.

Radiation-induced ROS production was also inhibited by disruptive *TP53*. In our study, inhibition of secondary ROS production several hours *after* the initial cellular insult by radiation had a dramatic effect on cellular senescence. This argues for prolonged ROS production following radiation playing a key role in the maintenance of the senescent phenotype. These ROS are most likely derived from the mitochondria and, in fact, we have previously observed decreased baseline mitochondrial complex activity in cells expressing C176F compared to wild type *TP53* (27). This argues for a suppressive effect on the mitochondria of disruptive *TP53*, which is relieved by inhibition of p53 expression. This offers a possible link between disruptive *TP53* mutations GOF and the inhibition of radiation-induced ROS and senescence. Theoretically, disruptive p53 could interact with known targets of wild type p53 involved in mitochondrial function, exerting an inhibitory function as opposed to the stimulation seen with wild type or some nondisruptive forms of *TP53*.

Our data strongly suggest that disruptive *TP53* portends poor clinical outcome in HNSCC associated with increased radioresistance. Parallel work in our laboratory has demonstrated that cells with disruptive *TP53* exhibit a therapeutically exploitable decrease in metabolic flexibility (27). One agent that can target this process is metformin. Recently, it has been shown that patients taking metformin have improved responses following neoadjuvant chemotherapy (51) and that metformin is a radiosensitizer *in vitro* (52). Metformin is hypothesized to affect mitochondrial function, and several studies have shown that it induces ROS in certain cellular backgrounds (37; 38). Also, it has been hypothesized that metformin may induce senescence in cells that are “senescence prone” (53). Interestingly, when we examined the effects of metformin *in vitro*, radiation-induced senescence and toxicity were potentiated only in cells expressing disruptive *TP53*, an effect that was modulated by altering p53 expression. This dramatic effect on the efficacy of radiation was also seen in our *in vivo* orthotopic model, as well as in patients taking metformin at the time of PORT.

Although this only included 10 patients in the metformin group, the reduction in LRR was profound and argues for the possibility of a dramatic clinical benefit with targeting of radiation-induced senescence.

The current study is limited by its retrospective nature, although the patient cohort includes a homogenous group of patients treated uniformly with surgery and PORT. Furthermore, the *in vitro* studies are limited by the analysis of a subset of disruptive and nondisruptive *TP53* mutations, and the possibility exists that other disruptive *TP53* mutations may behave differently. However, examination of a large panel of HNSCC cell lines confirmed the *in vitro* predictive value of the disruptive classification. Also, clinical data showing dramatically increased LRR in patients with disruptive *TP53* mutations supports the overall hypothesis. Although the disruptive category is empiric in nature, the fact that senescence appears to be strongly inhibited by these mutations allows further refinement. Specifically, testing of *TP53* mutants' ability to induce senescence could be performed, refining an already clinically predictive model. Finally, although the clinical data regarding the benefit of metformin is compelling, only a small number of patients were treated with the drug at the time of radiation. Despite the intriguing *in vitro*, *in vivo*, and clinical finding of radiation potentiation by metformin, these findings do not provide a definitive conclusion, but rather are hypothesis-generating and require additional validation.

Despite these limitations, we have demonstrated for the first time that disruptive *TP53* mutation predicts both LRR following PORT and *in vitro* response to radiation in HNSCC. Additionally, we have demonstrated that this effect is due to altered senescence and can be overcome using metformin, which appears to have dramatic clinical benefit.

Supplementary Material

Refer to Web version on PubMed Central for supplementary material.

Acknowledgments

The authors thank Mei Zhou and Samar Jasser for their assistance with basic laboratory work and logistics. The authors also thank Christina Dodge for her assistance with the *in vivo* experiments.

Funding

This work was partially supported by an American Society of Radiation Oncology Resident Seed Award; the U.T. M.D. Anderson Cancer Center PANTHEON program; National Institutes of Health Specialized Program of Research Excellence Grant P50CA097007; RO1 DE14613 National Institutes of Health; National Research Science Award Institutional Research Training Grant T32CA60374; and National Institutes of Health Program Project Grant CA06294 and Cancer Center Support Grant CA016672.

Glossary

ROS	reactive oxygen species
PORT	postoperative radiation therapy
LRR	locoregional recurrence
HNSCC	head and neck squamous cell carcinoma
NAC	N-acetyl cysteine

Bibliography

1. Jemal A, Bray F, Center MM, Ferlay J, Ward E, Forman D. Global cancer statistics. CA Cancer J Clin. 2011 Apr; 61(2):69–90. [PubMed: 21296855]
2. Agrawal N, Frederick MJ, Pickering CR, Bettegowda C, Chang K, Li RJ, et al. Exome sequencing of head and neck squamous cell carcinoma reveals inactivating mutations in NOTCH1. Science. 2011 Aug; 333(6046):1154–1157. [PubMed: 21798897]
3. Alsner J, Sørensen SB, Overgaard J. TP53 mutation is related to poor prognosis after radiotherapy, but not surgery, in squamous cell carcinoma of the head and neck. Radiother Oncol. 2001 May; 59(2):179–185. [PubMed: 11325447]
4. Koch WM, Brennan JA, Zahurak M, Goodman SN, Westra WH, Schwab D, et al. p53 mutation and locoregional treatment failure in head and neck squamous cell carcinoma. J Natl Cancer Inst. 1996; 88(21):1580–6. [PubMed: 8901856]
5. Thames HD, Petersen C, Petersen S, Nieder C, Baumann M. Immunohistochemically detected p53 mutations in epithelial tumors and results of treatment with chemotherapy and radiotherapy. A treatment-specific overview of the clinical data. Strahlenther Onkol. 2002 Aug; 178(8):411–421. [PubMed: 12240546]
6. Fallai C, Perrone F, Licitra L, Pilotti S, Locati L, Bossi P, et al. Oropharyngeal squamous cell carcinoma treated with radiotherapy or radiochemotherapy: prognostic role of TP53 and HPV status. Int J Radiat Oncol Biol Phys. 2009 Nov; 75(4):1053–1059. [PubMed: 19577857]
7. Poeta ML, Manola J, Goldwasser MA, Forastiere A, Benoit N, Califano JA, et al. TP53 mutations and survival in squamous-cell carcinoma of the head and neck. N Engl J Med. 2007; 357(25):2552–61. [PubMed: 18094376]
8. Perrone F, Bossi P, Cortelazzi B, Locati L, Quattrone P, Pierotti MA, et al. TP53 mutations and pathologic complete response to neoadjuvant cisplatin and fluorouracil chemotherapy in resected oral cavity squamous cell carcinoma. J Clin Oncol. 2010 Feb; 28(5):761–766. [PubMed: 20048189]
9. Erber R, Conradt C, Homann N, Enders C, Finckh M, Dietz A, et al. TP53 DNA contact mutations are selectively associated with allelic loss and have a strong clinical impact in head and neck cancer. Oncogene. 1998 Apr; 16(13):1671–1679. [PubMed: 9582015]
10. Williams JR, Zhang Y, Zhou H, Gridley DS, Koch CJ, Russell J, et al. A quantitative overview of radiosensitivity of human tumor cells across histological type and TP53 status. Int J Radiat Biol. 2008 Apr; 84(4):253–264. [PubMed: 18386191]
11. Cuddihy AR, Bristow RG. The p53 protein family and radiation sensitivity: Yes or no? Cancer Metastasis Rev. 2004 Dec; 23(3–4):237–257. [PubMed: 15197326]
12. Gupta N, Vij R, Haas-Kogan DA, Israel MA, Deen DF, Morgan WF. Cytogenetic damage and the radiation-induced G1-phase checkpoint. Radiat Res. 1996 Mar; 145(3):289–298. [PubMed: 8927696]
13. Kawashima K, Mihara K, Usuki H, Shimizu N, Namba M. Transfected mutant p53 gene increases X-ray-induced cell killing and mutation in human fibroblasts immortalized with 4-nitroquinoline 1-oxide but does not induce neoplastic transformation of the cells. Int J Cancer. 1995 Mar; 61(1): 76–79. [PubMed: 7705936]
14. Strasser A, Harris AW, Jacks T, Cory S. DNA damage can induce apoptosis in proliferating lymphoid cells via p53-independent mechanisms inhibitable by Bcl-2. Cell. 1994 Oct; 79(2):329–339. [PubMed: 7954799]
15. Pardo FS, Su M, Borek C, Preffer F, Dombkowski D, Gerweck L, et al. Transfection of rat embryo cells with mutant p53 increases the intrinsic radiation resistance. Radiat Res. 1994 Nov; 140(2): 180–185. [PubMed: 7938466]
16. Biard DS, Martin M, Rhun YL, Duthu A, Lefaix JL, May E, et al. Concomitant p53 gene mutation and increased radiosensitivity in rat lung embryo epithelial cells during neoplastic development. Cancer Res. 1994 Jul; 54(13):3361–3364. [PubMed: 8012950]
17. Eriksson D, Stigbrand T. Radiation-induced cell death mechanisms. Tumour Biol. 2010 Aug; 31(4):363–372. [PubMed: 20490962]
18. Brown JM, Attardi LD. The role of apoptosis in cancer development and treatment response. Nat Rev Cancer. 2005 Mar; 5(3):231–237. [PubMed: 15738985]

19. Vakifahmetoglu H, Olsson M, Zhivotovsky B. Death through a tragedy: mitotic catastrophe. Cell Death Differ. 2008 Jul; 15(7):1153–1162. [PubMed: 18404154]
20. Roninson IB, Broude EV, Chang BD. If not apoptosis, then what? Treatment-induced senescence and mitotic catastrophe in tumor cells. Drug Resist Updat. 2001 Oct; 4(5):303–313. [PubMed: 11991684]
21. Gudkov AV, Komarova EA. The role of p53 in determining sensitivity to radiotherapy. Nat Rev Cancer. 2003 Feb; 3(2):117–129. [PubMed: 12563311]
22. Castedo M, Perfettini J-L, Roumier T, Valent A, Raslova H, Yakushijin K, et al. Mitotic catastrophe constitutes a special case of apoptosis whose suppression entails aneuploidy. Oncogene. 2004 May; 23(25):4362–4370. [PubMed: 15048075]
23. Ianzini F, Bertoldo A, Kosmacek EA, Phillips SL, Mackey MA. Lack of p53 function promotes radiation-induced mitotic catastrophe in mouse embryonic fibroblast cells. Cancer Cell Int. 2006; 6:11. [PubMed: 16640786]
24. Merritt AJ, Allen TD, Potten CS, Hickman JA. Apoptosis in small intestinal epithelial from p53-null mice: evidence for a delayed, p53-independent G2/M-associated cell death after gamma-irradiation. Oncogene. 1997 Jun; 14(23):2759–2766. [PubMed: 9190891]
25. Lehmann BD, McCubrey JA, Jefferson HS, Paine MS, Chappell WH, Terrian DM. A dominant role for p53-dependent cellular senescence in radiosensitization of human prostate cancer cells. Cell Cycle. 2007 Mar; 6(5):595–605. [PubMed: 17351335]
26. Yigitbasi OG, Younes MN, Doan D, Jasser SA, Schiff BA, Bucana CD, et al. Tumor cell and endothelial cell therapy of oral cancer by dual tyrosine kinase receptor blockade. Cancer Res. 2004 Nov; 64(21):7977–7984. [PubMed: 15520205]
27. Sandulache VC, Skinner HD, Ow TJ, Zhang A, Xia X, Luchak JM, et al. Individualizing anti-metabolic treatment strategies for head and neck squamous cell carcinoma based on TP53 mutational status. Cancer. 2011 Jun 20. e-Pub ahead of print.
28. Eruslanov E, Kusmartsev S. Identification of ROS using oxidized DCFDA and flow-cytometry. Methods Mol Biol. 2010; 594:57–72. [PubMed: 20072909]
29. Rago R, Mitchen J, Wilding G. DNA fluorometric assay in 96-well tissue culture plates using Hoechst 33258 after cell lysis by freezing in distilled water. Anal Biochem. 1990 Nov; 191(1):31–34. [PubMed: 1706565]
30. el-Deiry WS, Tokino T, Velculescu VE, Levy DB, Parsons R, Trent JM, et al. WAF1, a potential mediator of p53 tumor suppression. Cell. 1993 Nov; 75(4):817–825. [PubMed: 8242752]
31. Sano D, Matsumoto F, Valdecanas DR, Zhao M, Molkentine DP, Takahashi Y, et al. Vandetanib restores head and neck squamous cell carcinoma cells' sensitivity to Cisplatin and radiation in vivo and in vitro. Clin Cancer Res. 2011 Apr; 17(7):1815–1827. [PubMed: 21350000]
32. Verheij M, Bartelink H. Radiation-induced apoptosis. Cell Tissue Res. 2000 Jul; 301(1):133–142. [PubMed: 10928286]
33. Catalano A, Rodilossi S, Caprari P, Coppola V, Procopio A. 5-Lipoxygenase regulates senescence-like growth arrest by promoting ROS-dependent p53 activation. EMBO J. 2005 Jan; 24(1):170–179. [PubMed: 15616590]
34. Macip S, Igarashi M, Fang L, Chen A, Pan Z-Q, Lee SW, et al. Inhibition of p21-mediated ROS accumulation can rescue p21-induced senescence. EMBO J. 2002 May; 21(9):2180–2188. [PubMed: 11980715]
35. Passos JF, Nelson G, Wang C, Richter T, Simillion C, Proctor CJ, et al. Feedback between p21 and reactive oxygen production is necessary for cell senescence. Mol Syst Biol. 2010; 6:347. [PubMed: 20160708]
36. Inoue T, Kato K, Kato H, Asanoma K, Kuboyama A, Ueoka Y, et al. Level of reactive oxygen species induced by p21Waf1/CIP1 is critical for the determination of cell fate. Cancer Sci. 2009 Jul; 100(7):1275–1283. [PubMed: 19432898]
37. Anedda A, Rial E, González-Barroso MM. Metformin induces oxidative stress in white adipocytes and raises uncoupling protein 2 levels. J Endocrinol. 2008 Oct; 199(1):33–40. [PubMed: 18687824]

38. Buzzai M, Jones RG, Amaravadi RK, Lum JJ, DeBerardinis RJ, Zhao F, et al. Systemic treatment with the antidiabetic drug metformin selectively impairs p53-deficient tumor cell growth. Cancer Res. 2007 Jul; 67(14):6745–6752. [PubMed: 17638885]
39. Goodwin WJ. Salvage Surgery for Patients With Recurrent Squamous Cell Carcinoma of the Upper Aerodigestive Tract: When Do the Ends Justify the Means? The Laryngoscope. 2000 Mar; 110(S93):1–18. [PubMed: 10714711]
40. Brown JM, Attardi LD. The role of apoptosis in cancer development and treatment response. Nat Rev Cancer. 2005 Mar; 5(3):231–237. [PubMed: 15738985]
41. Ewald JA, Desotelle JA, Wilding G, Jarrard DF. Therapy-Induced Senescence in Cancer. J Natl Cancer Inst. 2010 Oct; 102(20):1536–1546. [PubMed: 20858887]
42. Mattera L, Courilleau C, Legube G, Ueda T, Fukunaga R, Chevillard-Briet M, et al. The E1A-Associated p400 Protein Modulates Cell Fate Decisions by the Regulation of ROS Homeostasis. PLoS Genet. 2010 Jun.6(6)
43. Yu C, Rahmani M, Conrad D, Subler M, Dent P, Grant S. The proteasome inhibitor bortezomib interacts synergistically with histone deacetylase inhibitors to induce apoptosis in Bcr/Abl+ cells sensitive and resistant to STI571. Blood. 2003 Nov; 102(10):3765–3774. [PubMed: 12893773]
44. Wang B, Xiao Z, Ren EC. Redefining the p53 response element. Proc Natl Acad Sci USA. 2009 Aug; 106(34):14373–14378. [PubMed: 19597154]
45. Kato S, Han S-Y, Liu W, Otsuka K, Shibata H, Kanamaru R, et al. Understanding the function–structure and function–mutation relationships of p53 tumor suppressor protein by high-resolution missense mutation analysis. Proc Natl Acad Sci USA. 2003 Jul; 100(14):8424–8429. [PubMed: 12826609]
46. Jordan JJ, Inga A, Conway K, Edmiston S, Carey LA, Wu L, et al. Altered-function p53 missense mutations identified in breast cancers can have subtle effects on transactivation. Mol Cancer Res. 2010 May; 8(5):701–716. [PubMed: 20407015]
47. Dearth LR, Qian H, Wang T, Baroni TE, Zeng J, Chen SW, et al. Inactive full-length p53 mutants lacking dominant wild-type p53 inhibition highlight loss of heterozygosity as an important aspect of p53 status in human cancers. Carcinogenesis. 2006 Jul; 28(2):289–298. [PubMed: 16861262]
48. Jung Y-S, Qian Y, Chen X. Examination of the expanding pathways for the regulation of p21 expression and activity. Cell Signal. 2010 Jul; 22(7):1003–1012. [PubMed: 20100570]
49. Back JH, Rezvani HR, Zhu Y, Guyonnet-Duperat V, Athar M, Ratner D, et al. Cancer cell survival following DNA damage-mediated premature senescence is regulated by mammalian target of rapamycin (mTOR)-dependent inhibition of sirtuin 1. J Biol Chem. 2011 May 27; 286(21):19100–8. [PubMed: 21471201]
50. Brady CA, Jiang D, Mello SS, Johnson TM, Jarvis LA, Kozak MM, et al. Distinct p53 Transcriptional Programs Dictate Acute DNA-Damage Responses and Tumor Suppression. Cell. 2011 May; 145(4):571–583. [PubMed: 21565614]
51. Jiralerspong S, Palla SL, Giordano SH, Meric-Bernstam F, Liedtke C, Barnett CM, et al. Metformin and pathologic complete responses to neoadjuvant chemotherapy in diabetic patients with breast cancer. J Clin Oncol. 2009 Jul; 27(20):3297–3302. [PubMed: 19487376]
52. Sanli T, Rashid A, Liu C, Harding S, Bristow RG, Cutz J-C, et al. Ionizing radiation activates AMP-activated kinase (AMPK): a target for radiosensitization of human cancer cells. Int J Radiat Oncol Biol Phys. 2010 Sep; 78(1):221–229. [PubMed: 20615625]
53. Menendez JA, Cufí S, Oliveras-Ferraros C, Vellon L, Joven J, Vazquez-Martin A. Gerosuppressant Metformin: less is more. Aging (Albany NY). 2011 Apr; 3(4):348–362. [PubMed: 21483040]

Translational Relevance

The lack of clinically utilized biomarkers in head and neck cancer is a significant problem in moving toward more individualized therapy. *TP53*, the gene that encodes the protein p53, is by far the most commonly mutated gene found in head and neck cancer. However, this finding has not been clinically useful in guiding therapy. We have used a method of grading *TP53* mutation based upon predicted functionality of the resultant protein and shown that a particular class of mutation has a much higher rate of locoregional failure following radiotherapy as well as a much higher rate of *in vitro* radioresistance by inhibiting radiation induced cellular senescence. Furthermore, we show that these resistant cells can be selectively radiosensitized via the use of the anti-diabetic drug metformin. Finally, we show significant decreases in locoregional failure following radiation as well as improved survival in patients taking metformin. Thus, we provide a common marker for poor outcome in head and neck cancer as well as a novel means by which to target these aggressive tumors.

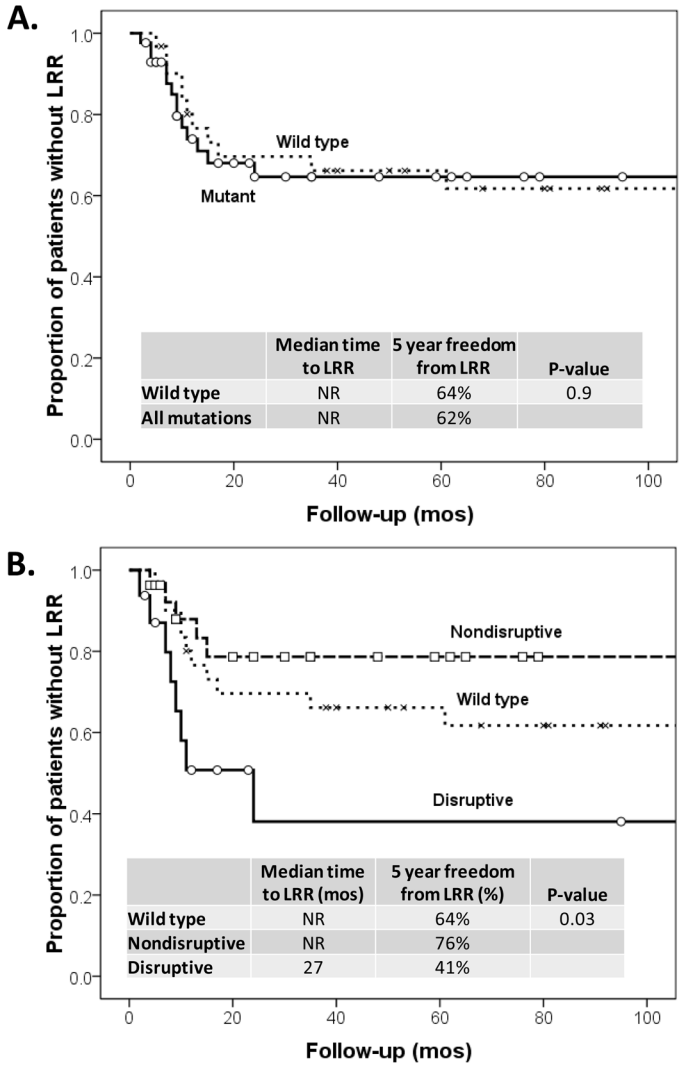

Figure 1. Locoregional Recurrence (LRR) occurs more frequently in patients with tumors expressing *TP53* disruptive mutations

(A) LRR in the study population in patients with either wild type *TP53* or any *TP53* mutation (p=0.9). (B) LRR in the same group of patients with the indicated *TP53* status.

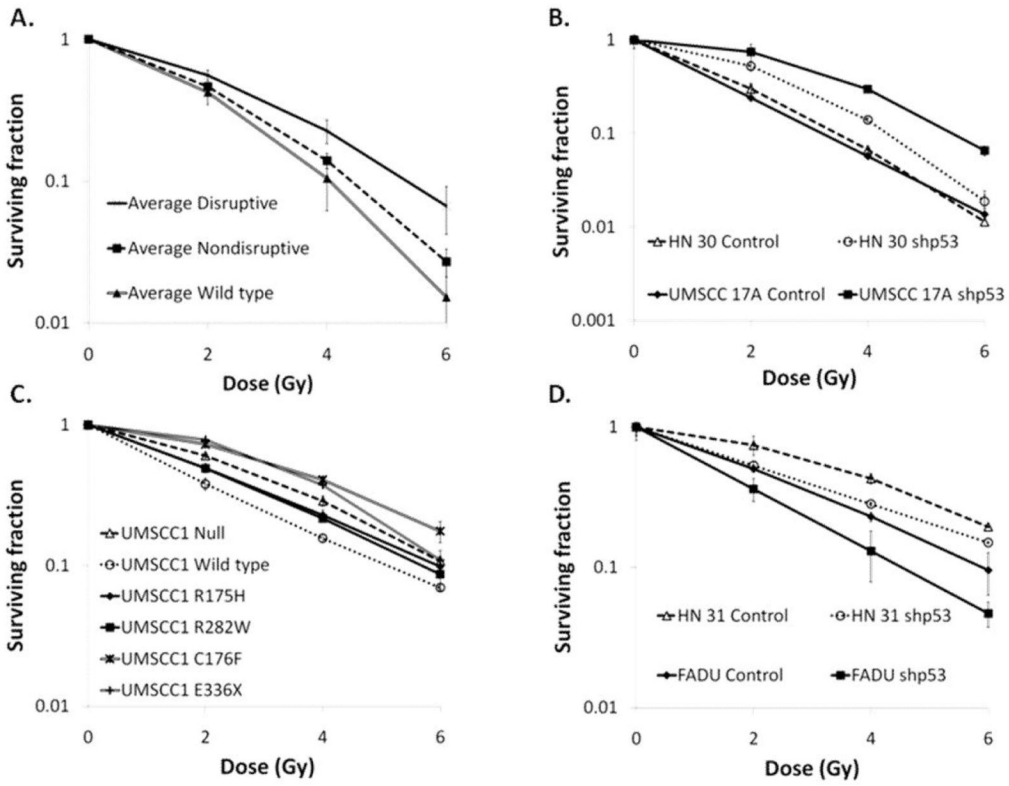

Figure 2. *In vitro* radiosensitivity is modulated by p53 expression depending on *TP53* classification

(A) A panel of 38 HNSCC cell lines was sequenced for *TP53* status and evaluated for radiosensitivity using standard clonogenic assays. Each cell line was then grouped by *TP53* status, and the average clonogenic survival data for each group is shown. (B) The effect of stable inhibition of wild type p53 expression (shp53) on radiosensitivity in HN 30 and UMSCC1 17A cells. (C) The effect of forced expression of wild type, R175H, R282W, or C176F *TP53* in p53 null UMSCC1 cells on radiosensitivity. (D) The effect of stable inhibition of p53 expression (shp53) on radiosensitivity in FADU and HN 31 cells (disruptive *TP53*).

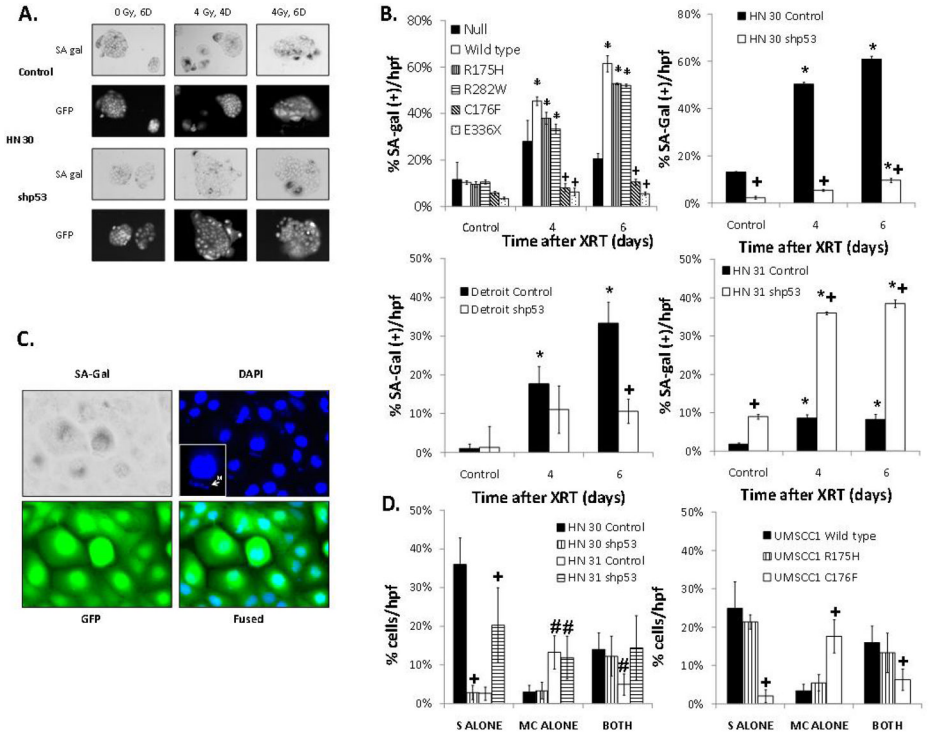

Figure 3. *TP53* modulates radiation-induced senescence, which correlates with radiosensitivity

(A) Representative light microscopy showing SA-Gal staining. (B) Percentage of SA-Gal positive cells per total number of cells in a high power field after 4 Gy of radiation for the times indicated in UMSCC1 cells expressing representative wild type and mutant *TP53* constructs and HN 30 (WT), Detroit (R175H) and HN 31 (C176F) where p53 is inhibited. (C) Representative microscopy showing SA-Gal staining, DAPI fluorescence, and GFP. (D) Percentage of cells either SA-Gal positive (S alone), exhibiting micronuclei (M alone) or both at 4 days after 4 Gy of radiation in HN 30 and HN 31 cells where p53 expression is inhibited and UMSCC1 cells expressing representative wild type and mutant *TP53* constructs. * - significantly elevated over baseline ($p<0.05$), + - significantly different from null at the indicated time point ($p<0.05$), # - significantly different from HN 30 control.

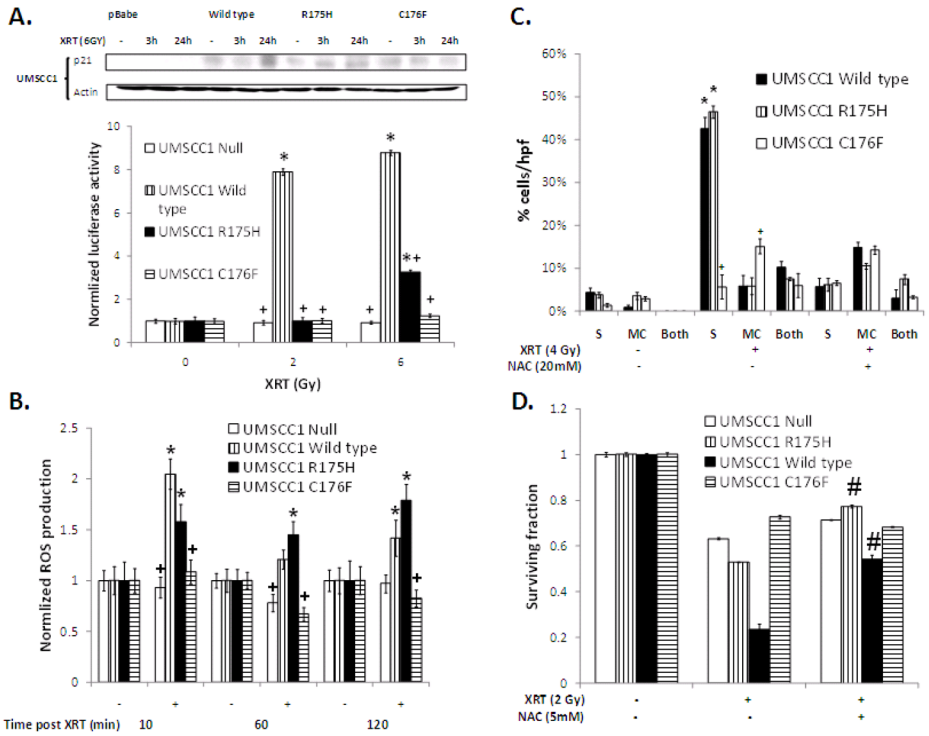

Figure 4. Radiation-induced senescence is associated with p21 expression and dependent on prolonged ROS production

(A) p21 protein expression and p21 luciferase reporter activity in UMSCC1 cells expressing the indicated *TP53* constructs treated with the indicated doses of radiation for 24h unless otherwise stated. (B) ROS production measured as indicated in the methods after 2 Gy of radiation. (C) Percentage of cells either SA-Gal positive (S alone), exhibiting micronuclei (MC alone) or both at 4 days after 4 Gy of radiation. Cells were treated with the indicated dose of NAC starting 2 h after radiation and treatment continued overnight. (D) Clonogenic survival after 2 Gy of radiation. Cells were treated with NAC in an identical manner to (C). * - significantly increased over unirradiated control ($p<0.05$), + - significantly different from UMSCC1 wild type in the same group ($p<0.05$). # - significantly increased compared to non-NAC treated group ($p<0.001$).

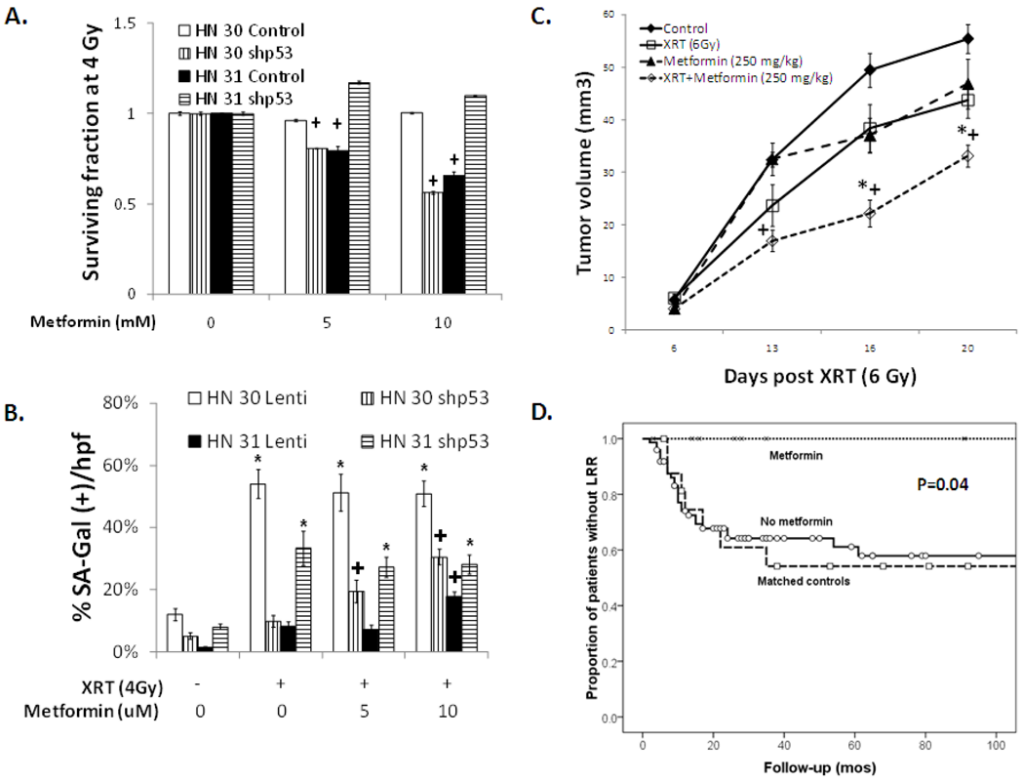

Figure 5. Metformin selectively radiosensitizes cells with disruptive *TP53* mutations, partially due to altered senescence

(A) Clonogenic survival after treatment with radiation at the indicated doses along with metformin for 24 hours in HN 30 and HN 31 cells in which p53 expression is inhibited using shRNA (shp53). (B) Percentage of SA-beta-gal positive cells per total number of cells in a high power field 4 days following 4 Gy of radiation and the indicated doses of metformin. * - significantly different from unirradiated control ($p<0.05$), + - significantly changed compared to no metformin treatment ($p<0.05$). (C) Tumor volume in mice with orthotopic tumors derived from HN 31 cells (C176F) after treatment with radiation (6 Gy), metformin (250 mg/kg, intraperitoneal) or both. * - significantly different from radiation alone ($p<0.05$), + -significantly different from metformin treatment alone ($p<0.05$). (D) LRR in patients taking metformin during treatment compared to the remainder of the study population as well as patients matched for tumor and nodal stage, surgical margin status, and *TP53* status to the metformin treated group ($p=0.04$).